

3D waveform simulation in Kobe of the 1995 Hyogoken-Nanbu earthquake by FDM using with discontinuous grids

S. Aoi

National Research Institute for Earth Science and Disaster Prevention

H. Sekiguchi, T. Iwata

Disaster Prevention Research Institute, Kyoto University

H. Fujiwara

National Research Institute for Earth Science and Disaster Prevention

ABSTRACT : We performed a simulation of the 1995 Hyogoken-Nanbu Earthquake with 3D finite-difference method (FDM) using discontinuous grids. In the waveform simulation using FDM, so long as we use the grids with uniform spacing for the calculation, the grid spacing is determined by the shortest wave length in the 3D simulation model space. In this study, we used discontinuous grids that consist of small grids (spacing of 50 m) in the region shallower than 2.6 km where there are low-velocity sedimentary layers, and coarse grids in the deeper region. In this way, we were able to reduce both the time and memory required for the computation to approximately 1/5 of what was needed in a calculation using small, uniform grids in the entire region.

1 INTRODUCTION

In Kobe, the most heavy damage of the 1995 Hyogoken-Nanbu Earthquake was distributed on a long zone and this is called the “Damaged Belt”. This particular distribution is due to the underground structure and the propagation of ruptures. Underground surveys using a reflection method or a refraction method were carried out after the earthquake, and the relatively detailed underground structure has been revealed (e.g. Huzita 1996). We also learned the details of the source process through inversions using data such as strong motion waveforms and geodetic data (e.g. Yoshida et al. 1996, Sekiguchi et al. 1998). Based on such information, 3D simulations were performed (e.g. Furumura & Koketsu 1998, Iwata et al. 1998, Kawase et al. 1998, Pitarka et al. 1998). These simulations underestimate the amplitude, although they do successfully explain the distribution of maximum amplitude qualitatively. One of the reasons is that their insufficient consideration of the low-velocity superficial layer (e.g. Iwata et al. 1998).

As long as we simulate the waveforms with the FDM using uniform grids, the grid spacing is determined by the shortest wave length in the model space. Hence, though the low-velocity layer exists only near the surface, we are still

obliged to use small grids. Thus it was difficult to introduce the low-velocity layer into the model, because of the drastic increasing of the grid number, in other words, required memory and computation time. Aoi & Fujiwara (1998a, b) formulated FDM using discontinuous grids that consist of small grids only near the surface where the low-velocity sedimentary layers exist, and coarser grids for the deeper region where the wave velocity is higher. This has shown to be very effective in reducing computing requirements. In this study, we applied this method to the 1995 Hyogoken-Nanbu Earthquake. A superficial layer with the S-wave velocity of 400 m/s, which is realistic according to the structure surveys, was introduced into the model in this study.

2 METHOD

We use discontinuous grids (Aoi & Fujiwara 1998b) that consist of staggered grids with two different grid spacing (Fig. 1). In Region I, the grid spacing is small (spacing h_1 is 50 m in this case), whereas in Region II, the spacing is three times coarser (spacing is $h_2=3h_1$). These two regions overlap in depth by $3h_1/2$. As to the terms of partial derivatives inside Regions I and II, we use the fourth-order finite-difference approximation

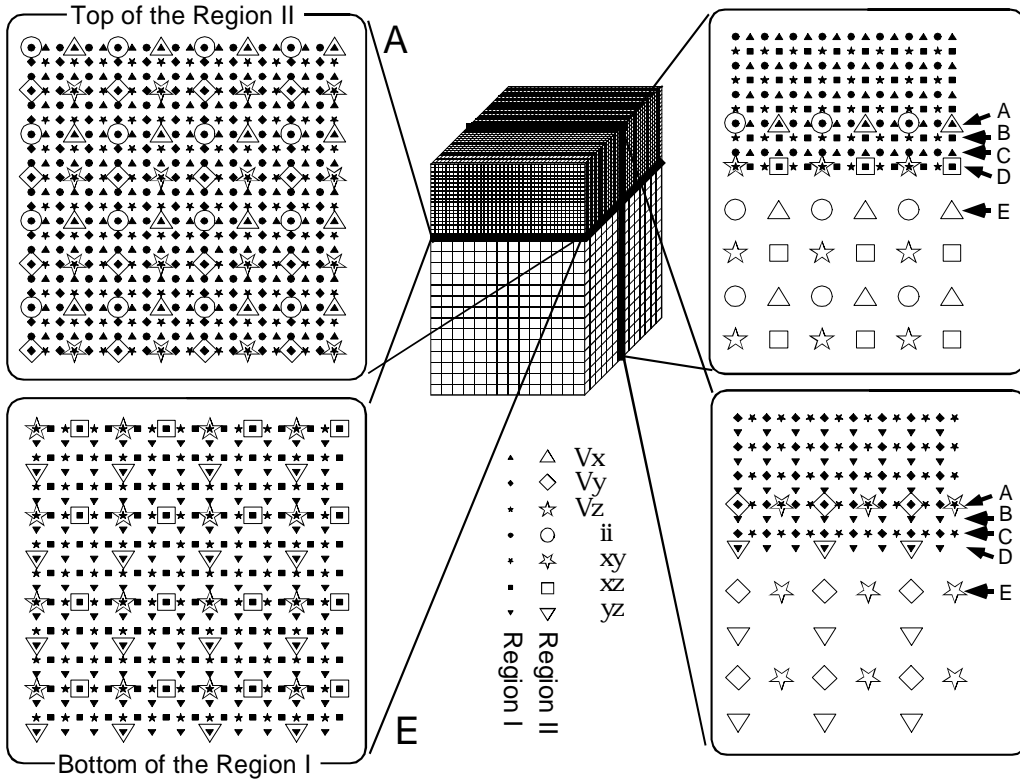


Fig.1 : (center) 3D discontinuous grid system. (left) Two transections on the top and at the bottom of the overlapping region of Regions I and II, where the elimination or the insertion of grids are necessary. (right) Two profiles of the discontinuous grids.

(e.g. Levander 1988), denoted as

$$f_i = \frac{1}{h} \{ c_0 (f_{i+1/2} - f_{i-1/2}) - c_1 (f_{i+3/2} - f_{i-3/2}) \} \quad (1).$$

(where $c_0 = 9/8$, $c_1 = 1/24$)

Here we cannot use the fourth-order finite-difference approximation for the term of partial derivatives concerning z in the adjacent region of the connecting region between Regions I and II. In such a region, we use the second-order finite-difference approximation (e.g. Virieux 1984),

$$f_i = \frac{1}{h} (f_{i+1/2} - f_{i-1/2}) \quad (2),$$

for the term of partial derivatives. In the connecting region between the two regions, we can calculate neither the velocities nor the stresses using the second-order finite-difference approximation (the left side of Fig. 1). Hence, these values are calculated by the linear interpolation and the elimination from the values of the other region. We should pay attention to the fact that we perform the interpolation and the elimination of all the variables within horizontal planes where the grid points concerned exist.

In order to minimize the artificial reflected waves from the boundary of calculation region, we use both the non-reflecting boundary condition of Cerjan et al. (1985) and the absorbing boundary

condition of Clayton and Engquist (1977).

3 UNDERGROUND STRUCTURE MODEL

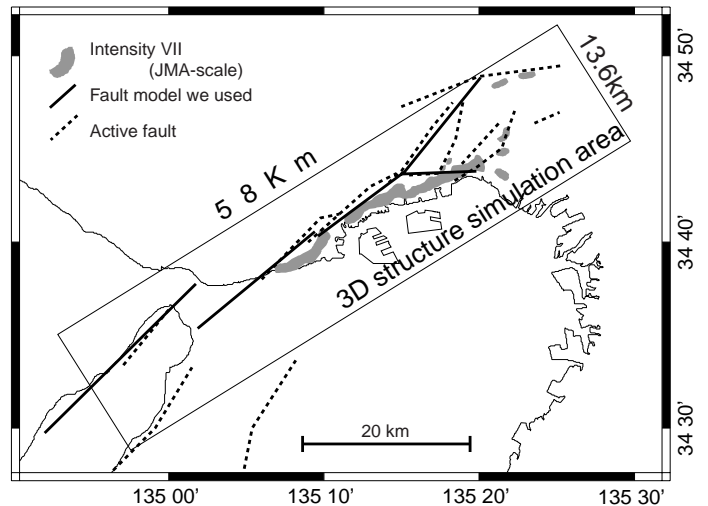


Fig. 2 : Map of Kobe area. The rectangle shows the area we are modeling in the study. The location of the heavily damaged zone is also shown [intensity VII, JMA scale, digitized by Koketsu (1997)]. The solid line shows the fault segment locations, and the dotted line shows active faults, traced by Huzita & Kazama 1983.

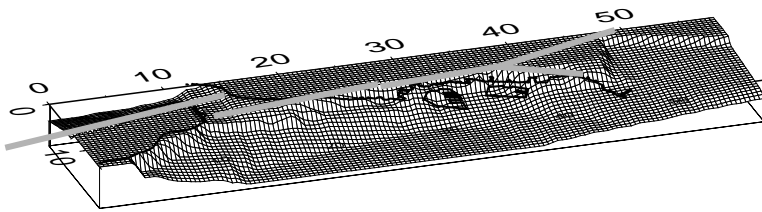


Fig. 3 : Bedrock topography in the Kobe area used in the 3D modeling. The shadow line shows the fault segment locations.

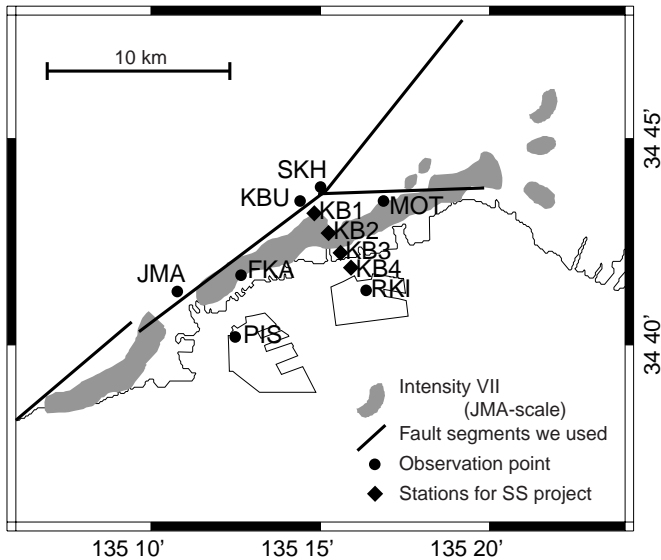


Fig. 4 : Map of observation points and the points designated by this simultaneous simulation project. The locations of fault segments and the heavily damaged zone are also shown.

Table 1. Model parameters.

	Model A	Model B
Sedimentary basin	Thickness = 50 % Vp = 2.0 km/s Vs = 0.6 km/s Dens. = 1.8 g/cm ³ Q = 80	Thickness = 16.7 % Vp = 1.8 km/s, Vs = 0.4 km/s Dens. = 1.75 g/cm ³ , Q = 60
		Thickness = 33.3 % Vp = 2.2 km/s, Vs = 0.8 km/s Dens. = 1.85 g/cm ³ , Q = 100
	Thickness = 50 % of sedimentary layer Vp = 2.4 km/s Density = 2.1 g/cm ³	Vs = 1.1 km/s Q = 120
Rock layer	Depth = ~ 4 km depth Vp = 5.5 km/s Density = 2.6 g/cm ³	Vs = 3.2 km/s Q = 300
	Depth = 4 km ~ 17.8 km depth Vp = 6.0 km/s Density = 2.7 g/cm ³	Vs = 3.46 km/s Q = 400
	Depth = 17.8 km depth ~ Vp = 6.7 km/s Density = 2.8 g/cm ³	Vs = 3.87 km/s Q = 500

In Kobe area, the underground structure has been investigated in detail using reflection and refraction methods and boring experiments (e.g. Huzita 1996). Using a bedrock shape estimated from this information, Pitarka et al. (1998) performed a simulation of 3D FDM using a model with homogeneous sedimentary layer. Iwata et al.

S. Aoi, H. Sekiguchi, T. Iwata & H. Fujiwara

Table 2. Locations of stations.

Station code	Latitude (N)	Longitude (E)	Station name
KBU	34.72500	135.24000	Kobe Univ.
MOT	34.72500	135.28100	Motoyama
SKU	34.73056	135.25000	Shinkobe Substation
PIS	34.67000	135.20800	Port Island Borehole
RKI	34.68877	135.27248	Rokko Island
FKA	34.69500	135.21083	Fukiai
JMA	34.68833	135.17944	JMA Kobe Station
KB1	34.720	135.247	Stations for SS project
KB2	34.712	135.254	
KB3	34.704	135.260	
KB4	34.698	135.265	

(1998) modified the bedrock topography of Pitarka et al. (1998), and divided its sedimentary layer into two layers of the same depth. We call the model of Iwata et al. (1998) Model A. The origin and the strike of the model are (34.584N, 134.881E) and N58E, respectively, and its size is 58.0 km (N58E), 13.6 Km (N148E), and 23.0 km (depth) (Fig. 2). Fig. 3 shows the bedrock topography of our models. The velocity structure of rock layer shown in Table 1 is from a structure model used for the hypocenter determination in this area by the RCEP-DPRI, Kyoto University. According to Iwata et al. (1998), although the use of the Model A and the source model of Sekiguchi et al. (1998) led to a successful representation of waveform characteristics, the amplitudes are underestimated. They point out that this is due to the effects of amplification caused by the superficial layer with low S-wave velocity, which is not taken into account sufficiently.

In this study, we use a model B where the upper sedimentary layer of the two layers of Model A is divided into two by 1:2 (Table 1). The S-wave velocity in the first and the second layers of Model B are 400 m/s and 800 m/s, respectively. This means that the interval velocity of these layers is identical to the S-wave velocity of the first layer of Model A, 600 m/s.

4 RESULT

4.1 Comparison with the observed waveforms

Fig. 4 shows the observation points where the data of the mainshock are available, the points designated by this simultaneous simulation project, and the areas severely damaged where the JMA intensity was VII (digitized by Koketsu 1997). KOB, KBU and SKH are the bedrock sites and the rest of observation points are located on the

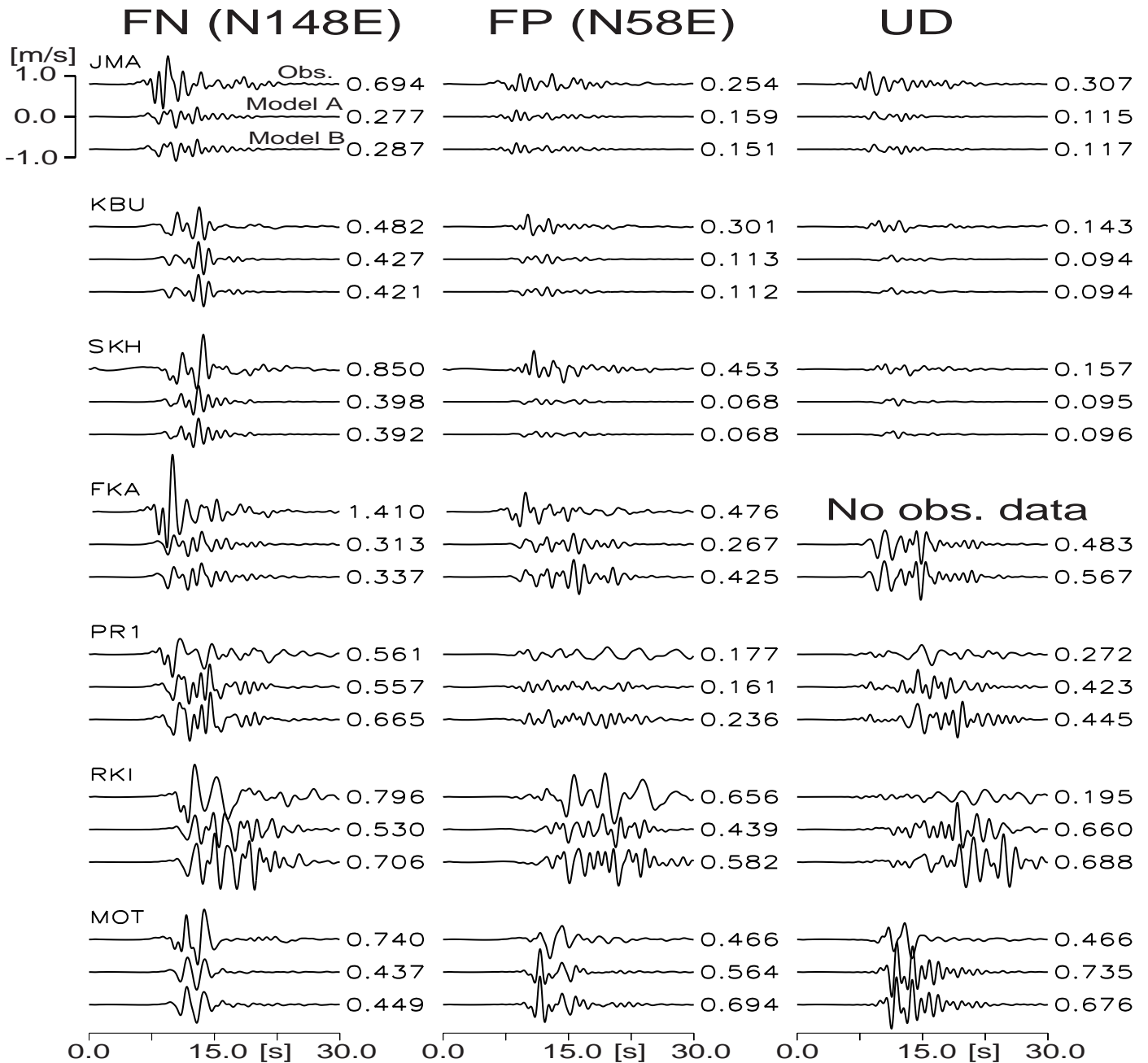


Fig. 5 : Comparisons between observed waveforms and synthetics of fault normal (N148E), fault parallel(N58E) and up-down components by Models A and B (0.1-1.0 Hz). The numbers on the right side of each trace shows the maximum amplitude in m/s.

sedimentary layer (Table 2). Fig. 5 shows the observed waveforms (0.1-1.0 Hz) of these observation points and the synthesized waveforms of Models A and B. The horizontal component of RKI and the fault parallel component of FKA were underestimated on the stations on the sedimentary layer in the simulation using Model A. In the simulation using Model B, the amplitude increased by approximately 30% and 70%, respectively, reproducing better the maximum amplitude of the observed waveforms. The bedrock sites such as SKH and JMA that gave the underestimated results logically do not show any improvement. On these stations, the weathering of the very superficial

granite might be causing the reduction of S-wave velocity. It is difficult to introduce such a thin layer into models even with the grids of 50 m that we used. The dominant periods of PR1 are not close to the observed waveform. This might be due to the effects of the very thin and soft superficial layer, and this is also difficult to introduce into models for the same reason.

4.2 Synthetics on KBU-RKI line

Fig. 6 shows the velocity waveforms (0.1Hz-1Hz) of two horizontal components as well as the maximum amplitude on each station of Models A

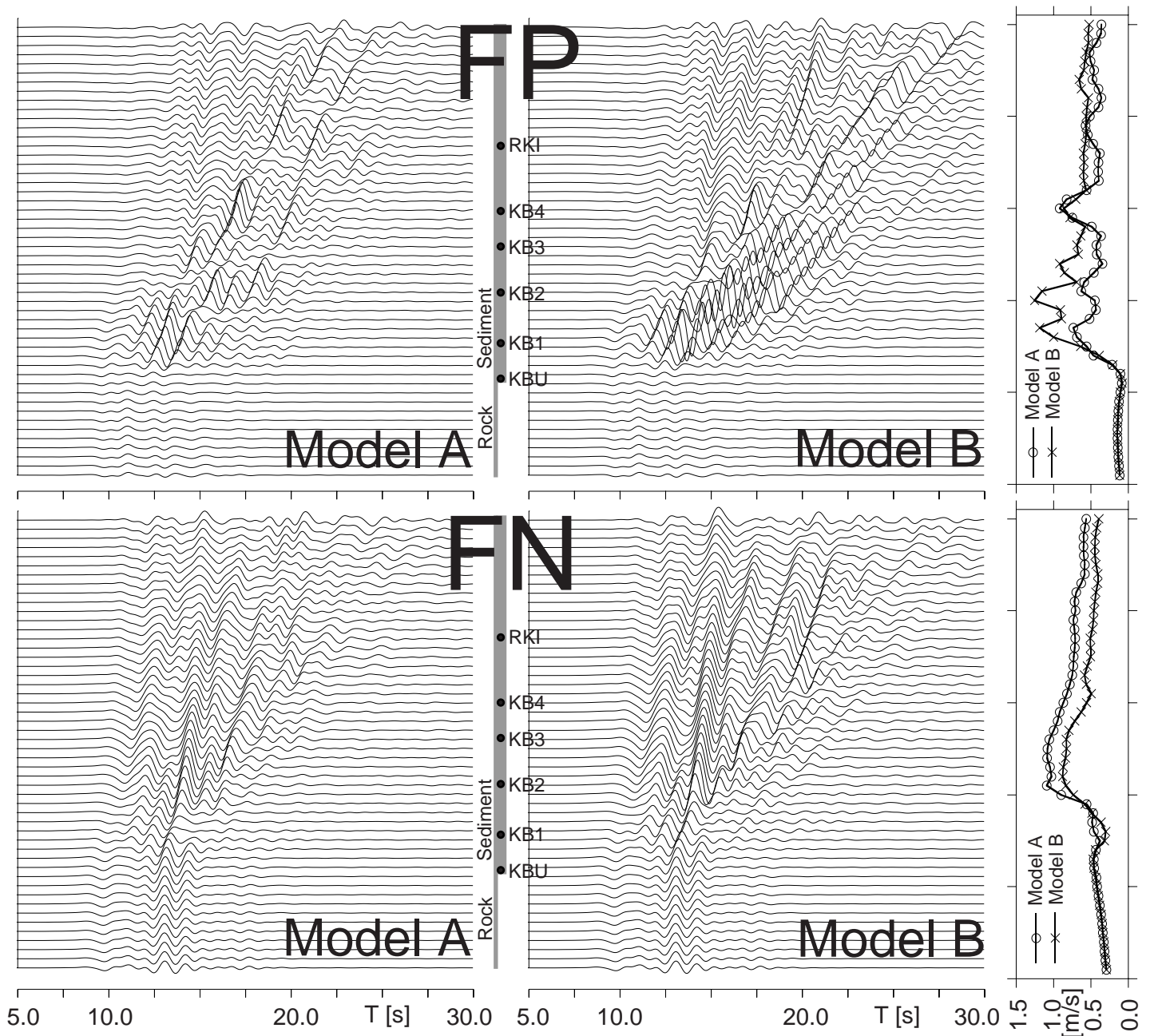


Fig. 6 : Synthetics of fault parallel and fault normal components by Models A and B on KBU-RKI line (0.1 - 1.0 Hz). The right side shows the maximum amplitude on each station by both models.

and B on KBU-RKI line. The waveforms of the two models on the rock sites match very closely, while the stations on the sediment show that the maximum amplitude of Model B is greater than that of Model A by approximately 20 – 100%.

KBU is on the boundary of the rock and the sediment, and the depth of the basement reaches 1km within 1km in south-east. In the zone between 1 km and 3 km from the rock, the maximum amplitude of fault parallel component by Model B exceeds 0.8 m/s. In addition to the amplification effect of soft sedimentary layer, this is also due to basin-edge effects. Slightly less than 1 km further in the south-east, the fault normal component exceeds 0.8 m/s, and still closer to the coast, the amplitude decreases gradually. The

width of the zone where the maximum amplitude of fault normal component exceeds 0.8 m/s is approximately 2.5 km. This zone of large amplitude corresponds to the “Damaged Belt”.

5 DISCUSSIONS AND CONCLUSIONS

We simulated strong ground motions in the source area during the 1995 Hyogoken-Nanbu Earthquake by fourth-order 3D FDM using discontinuous grids. Compared to the computation for same period range (0.1-1.0 Hz) with uniform grids, the discontinuous grids reduced the computational requirements to approximately 1/5. This leads to small grid spacing of 50 m in FDM calculation for

sedimentary layer. Using a structure model consisting of three sedimentary layers with the S-wave velocity of 400 m/s, 800 m/s and 1100 m/s, and a source model (Sekiguchi et al. 1998) which is applicable up to 1Hz, we simulated strong ground motions in the source area and compared with the observed waveforms on several stations. The maximum amplitudes of the horizontal components of RKI by Model B are larger by approximately 30% than those by Model A, they become almost the same level of those of the observed waveforms. At the stations on the sedimentary layer on the KBU-RKI line, we found that the maximum amplitudes by Model B against those by Model A are approximately 20-100% larger.

A thin superficial layer of less than 100-400 m thickness with the low S-wave velocity of 400 m/s influences even waveforms with relatively long period up to approximately 1Hz. The influence is not limited to the amplification by the low-velocity layer: it also influences the secondary generation and the propagation of the surface waves. Therefore, the influence of the superficial layer cannot be evaluated using 1D response functions. The existence of such superficial layers is confirmed by structure surveys, and their influence has to be taken into account when we synthesize waveforms even of relatively long period. The FDM using discontinuous grids is a very useful tool for a simulation considering the superficial layer of low velocity.

ACKNOWLEDGEMENT

Computation time was provided by the Supercomputer center of National Research Institute for Earth Science and Disaster Prevention. The data used here are collected and distributed by the Japanese Working Group on Effects of Surface Geology (ESG) on Seismic Motion, Association for Earthquake Disaster Prevention, for the Kobe Simultaneous Simulation Project during the second International Symposium on ESG 98. We used GMT Version 3 for figures.

REFERENCES

Aoi, S. & H. Fujiwara 1998a. 3-D finite-difference method using discontinuous grids, *Bull. Seism. Soc. Am.* (in printing).
 Aoi, S. & H. Fujiwara 1998b. 3-D Fourth-Order Finite-Difference Seismograms Using Discontinuous Grids, *Japan Earthquake Engineering Symposium Proceedings* (in printing).
 S. Aoi, H. Sekiguchi, T. Iwata & H. Fujiwara

(in printing).
 Cerjan, C., D. Kosloff, R. Kosloff, & M. Reshef 1985. A nonreflecting boundary condition for discrete acoustic & elastic wave equations, *Geophysics* 50: 705-708.
 Clayton, R. & B. Engquist 1977. Absorbing boundary conditions for acoustic & elastic wave equations. *Bull. Seism. Soc. Am.* 67: 1529-1540.
 Furumura, T. & K. Koketsu 1998. Specific distribution of ground motion during the 1995 Kobe earthquake and its generation mechanism, *Geophysical Research Letters*, 25: 785-788.
 Huzita, K. 1996. On survey results of active faults in Osaka-Kobe area, *Proc. 9th seminar on studying active faults, 'on deep structure of Osaka-bay area'*, 1-1 (in Japanese).
 Huzita, K. & T. Kazama 1983. Geology of the Kobe district. Quadrangle Series Scale 1:50,000, Geological Survey of Japan, Tsukuba, 115p (in Japanese).
 Iwata, T., H. Sekiguchi, A. Pitarka, K. Kamae & K. Irikura 1998. Evaluation of Strong Ground Motions in the Source Area, during the 1995 Hyogoken-Nanbu (Kobe) earthquake, *Japan Earthquake Engineering Symposium Proceedings* (in printing).
 Kawase, H., S. Matsushima, R.W. Graves & P.G. Somerville 1998. Strong Motion Simulation in Kobe with Special Reference to the Damage Belt Formation during the Hyogo-ken Nanbu Earthquake of 1995, *Japan Earthquake Engineering Symposium Proceedings* (in printing).
 Koketsu, K. 1998. An overview of the rupture process, *Report on the Hanshin-Awaji Earthquake Disaster, Common Series, 2*: 168-75. Tokyo: Maruzen (in Japanese).
 Levandar, A. R. 1988. Fourth-order finite-difference P-SV seismograms, *Geophysics* 53: 1425-1436.
 Pitarka, A., K. Irikura, T. Iwata & H. Sekiguchi 1998. Three-dimensional simulation of the near-fault ground motion for the 1995 Hyogoken-nanbu, Japan, earthquake, *Bull. Seism. Soc. Am.* 88, 428-440.
 Virieux, J. 1986. P-SV wave propagation in heterogeneous media: Velocity-stress finite-difference method, *Geophysics* 51: 889-901.
 Yoshida, S., K. Koketsu, B. Shibasaki, T. Sagiya & Y. Yoshida 1996. Joint inversion of near- and far-field waveforms and geodetic data for the rupture process of the 1995 Kobe earthquake, *J.*

